

Global Structure and Kinematics of the Spiral Galaxy NGC 2841

V. L. Afanasiev

Special Astrophysical Observatory, Nizhnij Arkhyz, 357147 Russia

Electronic mail: vafan@sao.ru

and

O. K. Sil'chenko¹

Sternberg Astronomical Institute, Moscow, 119899 Russia

Isaac Newton Institute, Chile, Moscow Branch

Electronic mail: olga@sai.msu.su

Received _____; accepted _____

arXiv:astro-ph/9812390v1 21 Dec 1998

¹Guest Investigator of the RGO Astronomy Data Centre

ABSTRACT

Investigation of gaseous and stellar kinematics and of broad-band VRI and narrow-band H_α and $[\text{NII}]\lambda 6583$ images is performed for the central part ($R < 4$ kpc) of the regular spiral galaxy NGC 2841. We have found emission-line splitting at $R < 20''$ and three-component LOSVD for the stars in the radius range $6'' \div 100''$. Morphological analysis reveals strong narrow shock fronts close to the major axis in the radius range of $30'' \div 50''$, a turn of the isophote major axis by 5° and strongly negative Fourier coefficient a_4 (boxy isophotes) in the radius range of $15'' \div 33''$. In principle, all these features may be explained in the frame of a triaxial bulge hypothesis.

Subject headings: galaxies: spiral — galaxies: individual (NGC 2841) — galaxies: kinematics and dynamics — galaxies: structure

1. Introduction

NGC 2841 is a regular early-type spiral galaxy, rather isolated, without any morphological signs of past interaction. It has a weak LINER nucleus (e.g., Ho et al. 1995) and a flocculent spiral structure (Elmegreen and Elmegreen 1982). We have investigated the innermost part of the galaxy inside $R = 10''$ with the Multi-Pupil Field Spectrograph of the 6m telescope (Sil’chenko et al. 1997). The stellar nucleus of NGC 2841 was found to be chemically decoupled, being more metal rich than surrounding bulge by a factor of 2.3; moreover, nuclear ionized gas demonstrated rotation in the plane strictly orthogonal to the global galactic plane (and to the rotation plane of stars in the center of the galaxy too). It looks like a small gaseous polar ring. Global polar rings are usually treated as signatures of past interaction with gas accretion or even of a minor merger. But such an event cannot affect only the very center of the galaxy; there must be any peculiarities in the global structure. We have found some hints on the presence of a dynamically decoupled stellar component in the bulge of NGC 2841 (Sil’chenko et al. 1997); but a further investigation of the global structure and kinematics of the galaxy was needed to understand what we see here.

NGC 2841 is known to possess a quite regular structure. The only claim about its peculiarity was result of Varela et al. (1996) that the bulge of NGC 2841 is a triaxial ellipsoid with varying axis ratio. Starting from the pioneer work of Zaritsky & Lo (1986), a triaxial bulge in a spiral galaxy is usually detected by a turn of isophote major axis at the galactic center. But the isophote major axis turn in NGC 2841, which causes Varela et al. (1996) to claim a presence of the triaxial bulge, is quite small, only 10° according to their measurements ($P.A. = 154^\circ$ for the bulge and $P.A. = 144^\circ$ for the disk). If we take into account a lot of other independent determinations of the line-of-nodes orientation in NGC 2841 (photometry: $P.A._0=147^\circ$, RC3, Moriondo et al. 1998, $P.A._0=150^\circ$, Heraudeau

and Simien 1996, Sil’chenko et al. 1997; neutral hydrogen kinematics: $P.A._0=150^\circ$, Rots 1980), this value may be even smaller, $4^\circ-7^\circ$, and then is comparable with the measurement errors. Besides, the orientation of the isophote major axis $P.A.=154^\circ$, which is ascribed to the triaxial bulge by Varela et al. (1996), is observed only in the radius range of $20''-40''$; closer to the center the $P.A.$ value falls to the outermost level, $P.A.=147^\circ$, and Varela et al. are forced to suggest a presence of ANOTHER inner bar aligned with the line of nodes to explain a behaviour of isophote position angle dependence on the radius. The structure begins to look too complex for such a small position angle variation. So, the question of triaxial bulge presence in NGC 2841 must be regarded more carefully by involving kinematical data for gas and stars in the central region dominating by the bulge potential. Our paper treats just this problem. A description of observational data used for the analysis is presented in Sec. 2. The kinematical results are discussed in Sec. 3, and the morphological results – in Sec. 4. Finally, in Sec. 5 we briefly discuss some details and conclude with a summary of our study.

2. Observational Data

The data which we analyse in this work include long-slit spectra taken almost along the major axis of NGC 2841, broad-band VRI panoramic photometry and narrow-band images obtained through the scanning Fabry-Perot interferometer in combination with interference filters centered on the redshifted emission lines H_α and $[\text{NII}]\lambda 6583$. We have used facilities of the La Palma Archive as well as our own observations made at the 6m telescope of the Special Astrophysical Observatory (Nizhnij Arkhyz, Russia).

Spectral data were obtained on January 6 and 7, 1991, at the 4.2m William Herschel Telescope on La Palma with the ISIS, red arm, equipped by a CCD 800×1180 . Two spectral ranges were exposed, $5830-6680 \text{ \AA}$ included the strongest emission lines H_α and

[NII] λ 6583 and 8000–8840 Å included the strongest stellar absorption lines Ca II λ 8498, 8542, 8662. The dispersion was 0.74 Å per pixel which corresponds to the spectral resolution of 2 Å, the slit width was 0".9, and a scale along the slit was 0".335 per pixel. The galaxy was exposed in two position angles, $P.A. = 145^\circ$ and 153° , both close to the major axis. Exposure times were set equal to 1 hour, except the exposure in $P.A. = 153^\circ$, 5830–6680 Å, which was of 40 min. Copper-neon and copper-argon comparison lamps were used for wavelength calibration; a check by measuring night-sky emission lines has shown that the inner accuracy of a single velocity measurement inside one spectrum frame is not worse than 2 km/s, though a systematic shift of the whole frame by 10–30 km/s is possible between neighboring exposures. Two bright stars, HR 3125 (K1III) and HR 3222 (G8III), were used as templates for a cross-correlation in the spectral range of 8000–8840 Å to obtain stellar velocities along the major axis of NGC 2841.

The photometric data were obtained on May 6, 1988, at the 1m Jacobus Kapteyn Telescope on La Palma with CCD 385×578 , through the broad-band filters VRI . A spatial scale was 0".30 per pixel, so only the central part of the galaxy was exposed; the seeing quality ($FWHM$) was 0".7–0".8. The exposure times were 300+300 sec (V), 300+200 sec (R), and 200+200 sec (I). No photometric standards were observed, so we have not made any attempts to calibrate these CCD frames. Instead we have made an isophotal analysis deriving radial dependencies of the major-axis position angle, isophote ellipticity, and boxiness.

At the 6m telescope we have observed NGC 2841 with the scanning Fabry-Perot interferometer (Dodonov et al. 1995) twice: in December 1996 in the emission line H_α and in May 1997 in the emission line [NII] λ 6583. The observations were undertaken in the frame of the project of Prof. A. M. Fridman dedicated to a search of large-scale vortices in gas velocity fields of spiral galaxies. Here we present only narrow-band images of NGC 2841 in

H_α and [NII] emission lines obtained as by-products of these observations. A CCD detector with format of 1060×1180 was used with a binning of 2×2 ; a resulting scale of $0''.455$ per pixel after binning 2×2 allowed to register an area of $4' \times 4'.5$. The seeing quality was $2''.3$ in December 1996 and $1''.7$ in May 1997.

All the observational data were reduced by using the software developed in the Special Astrophysical Observatory (Vlasyuk 1993) and the software ADHOC developed in the Marseille Observatory (Boulesteix 1993).

3. Kinematical Results

3.1. Gas line-of-sight velocity distributions

The long-slit spectra obtained in the spectral range of 5830–6680 Å reveal a presence of quite measurable emission lines H_α and [NII] in the full radius range of $0'-2'$ covered by the observations. Inside $R = 60''$ the nitrogen emission line $\lambda 6583$ is almost everywhere stronger than H_α implying a shock excitation mechanism; sometimes the emission lines are clearly splitting with a velocity separation of the components up to 150 km/s. We have measured gas line-of-sight velocities along the slit by searching for line baricenters and by applying a Gauss analysis to the multi-component profiles; the complete results are presented in Fig. 1, and the results for the central part are presented in Fig. 2. Outside $R \approx 50''$ the measured velocity distributions are quite regular, the rotation curve looks flat, in accordance with numerous previous investigations, at the level of $v_{rot} = 313$ km/s assuming after Whitmore et al. (1984) galaxy inclination to be 65° . In the inner part of NGC 2841, particularly inside $R \approx 20''$, the behaviour of the gas line-of-sight velocities is so complex that we cannot explain all the details of the velocity profiles. But some typical features of the distributions can be interpreted as evidences for a bar-like potential. First of all, though

the cross-sections in $P.A. = 145^\circ$ and in $P.A. = 153^\circ$ are positioned very tightly, Fig. 2a and Fig. 2b look quite different. It means that the structure in the center of NGC 2841 which causes the emission line splitting is very subtle, almost one-dimensional. Though the global disk of NGC 2841 is moderately inclined to the line of sight, by some 60° – 65° (Varela et al. 1996, Moriondo et al. 1998), it seems that we see a bar aligned with the line of nodes through the rotating gaseous disk. In $P.A. = 153^\circ$ (Fig. 2a) we can note two straight segments of the velocity distributions separated by 150–180 km/s in the same radius range, namely, $10''$ – $20''$ to the north from the center. It looks like a simultaneous registration of a fast-rotating gaseous disk and of a slow-rotating bar edge which is traced by gas radiating in a shock wave. A similar emission-line splitting has been predicted in the dynamical work of Kuijken and Merrifield (1995) who have considered visible effect of edge-on bars on major-axis line-of-sight velocity profiles. In $P.A. = 145^\circ$ (Fig. 2b) two straight segments have an opposite slope and are located in the radius ranges of $0''$ – $10''$ to the south and $10''$ – $20''$ to the north from the center. This configuration with a visible velocity break in the center of the symmetry can be understood if we remind that there exists a radius range (usually between two ILRs) where any bar provokes a predominance of gas orbits elongated orthogonally to this bar (e. g. Mulder 1986). The orbits highly elongated along the line of sight (seen "end-on") would provide just the configuration similar to that in Fig. 2b. Solely, a position of the velocity distribution symmetry center in this configuration must be shifted by $5''$ to the north from the photometric center. But it is quite possible: in our previous investigation (Sil'chenko et al. 1997) made with the panoramic spectrograph providing a two-dimensional velocity field we have already obtained a position of the symmetry center of the gas velocity field shifted to the north with respect to the brightness center position.

3.2. Stellar line-of-sight velocity distributions

We have derived stellar line-of-sight velocities by cross-correlating sky- and continuum-subtracted near-infrared galactic spectra line-by-line with the spectra of the template stars observed the same night. An example of the cross-correlation peaks is presented in Fig. 3. In the full radius range where the cross-correlation peaks are measurable – from $45''$ to the south from the nucleus toward $100''$ to the north – they demonstrate a multi-component structure. Velocity differences between the components are sufficiently large so extraction of the components is a procedure easy enough. We have used a Gauss analysis for this purpose. Curiously, as it is illustrated in Fig. 3a, to the south from the nucleus the intermediate-velocity component is the strongest one, and to the north from the nucleus, at $R > 25''$, the extremely blueshifted component becomes the most prominent. This asymmetry is the first sign of a triaxial bulge. Unfortunately, we have not been able to trace stellar velocity distributions toward the center of NGC 2841: inside $R \approx 6''$ stellar velocity dispersion strongly increases (or additional kinematical components arise?), and an unambiguous component separation becomes impossible. Beyond $R \approx 6''$ all the cross-correlation peaks can be decomposed mainly into three components; the corresponding three kinematical subsystems are presented in Fig. 4. Attached error bars characterize differences between velocity determinations by using two different template stars.

Unlike the gaseous velocity distributions in Fig. 1, the stellar velocity distributions in two different position angles, 145° and 153° , are quite identical. In Fig. 4 we see three stellar kinematical subsystems – two prograde and one retrograde. Among two prograde subsystems, one rotates by a factor of 3 faster than another. The rotation velocities of the slow-rotating prograde system and of the retrograde system are comparable. We have called these three subsystems "direct bulge", "disk", and "retrograde bulge". The rotation velocity of the disk is practically equal to the rotation velocity of the gaseous disk, so we

conclude that it is a dynamically cold stellar subsystem. The semi-amplitudes of velocity variations for the both "bulges" are of order of 100 km/s; and we cannot prove that the rotation of these components is circular. In the context of a triaxial bulge hypothesis an existence of two "bulge" kinematical subsystems is easily explained if the bulge is triaxial, seen edge-on, and slightly tumbling; in this case we see streaming stellar motions along the bar simultaneously in both directions.

4. Morphological Signatures of the Bar

4.1. Narrow-band H_α and [NII] images

Figure 5 presents isophotes of the surface brightness distributions in the emission lines H_α (a) and [NII] λ 6583 (b) for the very center of NGC 2841 $30'' \times 30''$. Earlier we have already constructed an analogous map in [NII] by using the observational data obtained with the Multi-Pupil Field Spectrograph of the 6m telescope (Sil'chenko et al. 1997); an agreement of the Fig. 5b presented here with the Fig. 11 in the previous work (Sil'chenko et al. 1997) is perfect even in details: again we see that the overall intensity distribution is aligned with the line of nodes ($P.A._0 = 150^\circ$), again we can notice an extra-component to the north from the nucleus aligned in $P.A. \approx 50^\circ$, and even splitting southern "tail" of the surface brightness distribution is exactly reproduced. Interestingly, the H_α image of the center of NGC 2841 (Fig. 5a) has appeared to be quite different: it is much more symmetric than the [NII] λ 6583 image though it demonstrates also some small peculiarities, such as concaves of the outer isophote at the $P.A. \approx 70^\circ$ (dust lane?). A lack of resemblance between the two images promises something interesting if mapping [NII]-to- H_α emission line ratio.

Figure 6 presents a full-format map of [NII] λ 6583 to H_α flux ratio with superimposed

isophotes of the H_α image. The map is normalized to the value $[\text{NII}]/H_\alpha=2$ in the nucleus which was obtained from the La Palma long-slit spectra. First of all, we can notice that in the spiral arms which are clearly sketched by the H_α emission maxima the $[\text{NII}]$ to H_α ratio falls below 0.5. It is consistent with an excitation of the ionized gas by hot massive stars. But besides the spiral arms, which are distinct by the low $[\text{NII}]$ -to- H_α ratio, there are also two long, slightly curved loci, which are distinct by a high $[\text{NII}]$ -to- H_α ratio. These features are located in the radius range of $30''$ – $50''$; their $[\text{NII}]/H_\alpha$ values between 3 and 4 allow to regard them as shock wave fronts. Their morphology resembles that of dust lanes which are often seen on the edges of bars and which are also related to shock wave fronts. Another evidence for a shock origin of the high $[\text{NII}]/H_\alpha$ ratio regions is presented in Fig. 7. The slit at the position angle $P.A. = 153^\circ$ crossed the southern feature at $R \approx 40''$ and $R \approx 50''$. Figure 7 shows a corresponding piece of the gas velocity curve. The nitrogen emission line in the radius range of $-54'' \div -38''$ has a double-peaked profile. We have fitted it by two Gaussians; one of them has given velocities corresponding to the regularly rotating disk, the second – the velocities smaller by some 100 km/s. This velocity splitting is a sure signature of shock waves.

4.2. Broad-band *VRI* photometry

A detailed surface photometry through the broad-band filters was already performed for NGC 2841 by Varela et al. (1996). They have used CCD observations from the 4.2m WH Telescope of La Palma taken under good seeing conditions. The data presented here are obtained at the much smaller telescope, but also under very good seeing conditions, so the quality of our morphological results has appeared to be not worse than in their work. Figure 8 presents radial dependencies of isophote major axis position angle, of isophote ellipticity, and of the fourth Fourier coefficient a_4 called "boxiness". The former

two dependencies at $a > 5''$ agree perfectly with the results of Varela et al. (1996); the boxiness was not analysed by them. The major axis position angle shows small variations over the full radius range under consideration; the central increase of $P.A.$ toward 156° must be real because of agreement with the results of our analysis of HST/WFPC image for NGC 2841 (Sil'chenko et al. 1997). Besides the $P.A.$ increase in the very center, we have also a plateau of $P.A.$ in the radius range of $13''$ – $35''$ at the level of $P.A. \approx 154^\circ$; outside this radius range the isophotes are aligned with the line of nodes. Varela et al. (1996) have obtained the same plateau in the same radius range and have interpreted it as a signature of bulge triaxiality. We agree because the same radius range is distinguished in Fig. 8c by strongly negative a_4 values in the all three filters. It is quite consistent with a picture of the large-scale bar seen edge-on implied by the kinematics (see the previous Section), because numerical studies of orbit instabilities have shown that barred galaxies must have boxy bulges (e. g. Pfenniger 1985). Inside $R \approx 12''$ the situation is not so clear: the major axis position angle coincides with that of the line of nodes, and a_4 is only mildly negative. Varela et al. (1996) suggested the second, inner bar, but for this hypothesis there are no arguments: their reference to Keel (1983) is erroneous, because Keel (1983) claimed a one-sided GASEOUS bar in the center of NGC 2841, not a two-sided stellar one. Perhaps it would be more correct to classify a zone of $R=4''$ – $12''$ as a transition from a slightly warped nuclear disk with a radius of $2''$ to the (possibly torus-like?) triaxial bulge. A behaviour of the isophote ellipticity (Fig. 8b) demonstrates characteristic oscillations which may result from the presence of two radially limited oblate components.

5. Discussion and Conclusions

The information which we have obtained on the kinematics of gas and stars in NGC 2841 is rich and somewhat unexpected. The ionized-gas emission lines are doubling

mainly inside $R = 20''$; but the stellar LOSVD is multi-component up to $R = 100''$! The stellar rotation inside $R = 40''$ in NGC 2841 was once investigated by Whitmore et al. (1984): two long-slit cross-sections, along $P.A. = 150^\circ$ and along $P.A. = 60^\circ$, were obtained under a spectral resolution of 3.4 \AA , that is twice worse than ours, and no subsystem multiplicity were noticed. As for gas rotation in this region Whitmore et al. (1984) said, with the reference to Rubin and Thonnard (private communication), that the innermost measurable emission was detected at $R = 52''$, and for the inner disk the rotation curve was extrapolated from this point to the center. The mean major-axis stellar velocity distribution of Whitmore et al. (1984) showed a prominent minimum at $R = 11''$; the velocity decrease was measured to be steeper than a Keplerian one, and Whitmore et al. (1984) accepted a triaxiality of the bulge. The bulge rotation velocity projected on the line of sight was estimated by them (after subtracting the extrapolated disk) as $70 \pm 30 \text{ km/s}$. This estimate seems to be quite reasonable: by the direct subsystem decomposition we have measured $v_{rot}^{los} = 106 \text{ km/s}$ for the "direct" bulge and 76 km/s for the "retrograde" bulge.

Here we must mention that our direct measurement of the bulge rotation curve is not unique. For example, Wagner et al. (1989) had presented two parallel rotation curves for the disk and bulge of NGC 4594 up to $R = 40''$; they have noticed that correlation peaks were doubling and, trying to decompose them with a lot of precautions, they have obtained two stellar subsystems, both cold enough, one of which rotated with the velocity of $\sim 300 \text{ km/s}$, and the other – slower by 120 km/s . The words "disk" and "bulge" were pronounced in their Discussion. But in NGC 4594 there were no any "counterrotating" subsystem which is seen, as third by its luminosity, in NGC 2841.

A counterrotating subsystem was reported to be found in another early-type spiral galaxy, NGC 7217, by Merrifield & Kuijken (1994). They have measured a double-peaked LOSVD and have claimed a discovery of two counterrotating stellar disks in NGC 7217;

they argued that outside $R = 10''$ a bulge contribution in this galaxy is negligible and cannot affect the measured stellar kinematics. But their photometric arguments were wrong: Buta et al. (1995) have decomposed a high-quality surface brightness profile of NGC 7217 and have found that a de Vaucouleurs' bulge dominates in this galaxy over the whole radius range. So perhaps in NGC 7217 Merrifield & Kuijken (1994) saw just the same "prograde" and "retrograde" bulges as we have seen in NGC 2841. Searching for a cause of multi-ring structure in NGC 7217, Buta et al. (1995) have also detected a slight triaxiality of the galaxy bulge; it implies that the hypothesis of elliptical stellar streams may be a quite reasonable explanation of what Merrifield & Kuijken (1994) saw in NGC 7217.

If we summarize the results of this work and those of our first paper (Sil'chenko et al. 1997) on NGC 2841, we obtain a curious list of kinematical and morphological features which must be jointed in the frame of one hypothesis. All of them are schematically shown in Fig. 9. These are:

- the most prominent photometric appearance of a bar in the radius range of $15''$ – $33''$;
- a presence of strong shocks on the trailing sides of the photometric bar in the radius range of $30''$ – $50''$;
- in the radius range of $5''$ – $15''$ gas is on orbits in the galactic plane but elongated orthogonally to the bar;
- inside $R \approx 5''$ gas rotates in the plane orthogonal to the galactic plane (Sil'chenko et al. 1997);
- the visible center of gas rotation is shifted by $3''$ – $5''$ to the north along the major axis with respect to the brightness center (Sil'chenko et al. 1997, this paper);
- star motions in the radius range of $4''$ – $10''$ have a significant line-of-sight velocity

component along the galaxy minor axis – either a polar ring or elongated plane orbits orthogonal to the bar (Sil’chenko et al. 1997);

- in the radius range of $10''$ – $100''$ we see two ”counterrotating” stellar bulges, moreover, to the north-west from the center we see them both through the stellar disk – the picture is consistent with elliptical streaming of stars along the photometric (but much shorter!) bar.

During the last two decades there were a lot of papers on gas response to an ovally distorted potential. Though the results seem to be model dependent, however some things are firmly established. We know, for example, that shocks at the trailing edges of a bar are a signature of the low contrast of the oval potential distortion (Matsuda et al. 1987) and that plane orthogonal orbit family dominates inside ILR (e. g. Mulder 1986). The most prominent theoretic bar manifestation in the gaseous disk must be perhaps two-armed spiral pattern – global density waves. Though NGC 2841 is a flocculent spiral galaxy, recently two smooth (grand-design?) spiral arms have been detected by Block et al. (1996) on the K' ($2.1\mu\text{m}$) image of this galaxy. The arms look dark; Block et al. (1996) suppose that they are density waves in the dust-gaseous disk of the galaxy. Therefore, these arms are just what must accompany the global bar which we report in this paper. Interestingly, NGC 2841 is not the only flocculent galaxy which demonstrates two-armed grand design spirals in the K' band; Thornley (1996) has found them in three flocculent galaxies of four ones which were investigated, and Grosbol and Patsis (1998) report several more objects of this kind. One of the galaxies, NGC 5055, has been studied in detail by Thornley and Mundy (1997); the infrared spiral arms have appeared to demonstrate also HI and CO concentrations and prominent gas streaming motions. So, global density waves are perhaps frequent enough in the gaseous disks of flocculent galaxies, and nothing prevents flocculent galaxies to possess triaxial bulges.

Another feature of gas behaviour found by us – nuclear gaseous ”polar ring” (Sil’chenko et al. 1997) – is not predicted by detailed dynamical simulations of bars because these simulations are mostly two-dimensional, and here we need to involve z direction. But there was an interesting observational note of Sofue and Wakamatsu (1994); they have seen an asymmetrical dust lane orthogonal to the global bar in the center of face-on SB galaxy M 83. Their physical arguments in favor of polar orbit predominance for the nuclear gas of barred galaxies are convincing enough.

Theoretical predictions of bar effects on stellar kinematics do not contradict our results too. The two bulge kinematical subsystems, prograde and retrograde, can be explained either by specific projection of elliptical streamlines of stars in the triaxial potential or by a presence of retrograde orbits in the triaxial potential: e. g., the recent dynamical investigation of Wozniak and Pfenniger (1997) has shown that in different models from 15% to 30% (by mass) stars of a bar are on retrograde orbits. Perhaps, a set of phenomena which we have derived here for NGC 2841 is sufficient for specialists in dynamics to build a model of the triaxial bulge in this galaxy and to answer if we can explain the whole phenomena in the frame of this model or some merger events must be involved.

We are grateful to Prof. A. M. Fridman for a permission to use the observational data obtained in the frame of his observational project prior to publication. We thank the astronomers of the Special Astrophysical Observatory Drs. S. N. Dodonov, V. V. Vlasyuk, and A. N. Burenkov for providing the observations at the 6m telescope with the scanning Fabry-Perot interferometer, and we thank Drs. V. V. Vlasyuk and J. Boulesteix from the Marseille Observatory for the possibility to use their data reduction programs. We are also grateful to Dr. R. Peletier who has attracted our attention to the observational data on NGC 2841 which are kept in the La Palma Archive. This research has made use of the La Palma Archive. The telescopes WHT and JKT are operated on the island of La Palma by

the Royal Greenwich Observatory in the Spanish Observatorio del Roque de los Muchachos of the Instituto de Astrofísica de Canarias. The 6m telescope is operated under the financial support of Science Department of Russia (registration number 01-43). The work was supported by the grant of the Russian Foundation for Basic Researches 98-02-16196 and by the Russian State Scientific-Technical Program "Astronomy. Basic Space Researches" (the section "Astronomy").

REFERENCES

- Block, D. L., Elmegreen, B. G., and Wainscoat, R. J. 1996, *Nature*, 381, 674
- Boulesteix, J. 1993, *ADHOC Reference Manual*. Marseille: Publ. de l'Observatoire de Marseille.
- Buta, R., van Driel, W., Braine, J., Combes, F., Wakamatsu, K., Sofue, Y., and Tomita, A. 1995, *ApJ*, 450, 593
- Dodonov, S.N., Vlasyuk, V.V., Drabek, S.V. 1995, *Fabry-Perot Interferometer Manual*. Nizhnij Arkhyz: SAO Publ.
- Elmegreen, D. M. and Elmegreen, B. G. 1982, *MNRAS*, 201, 1021
- Grosbol, P.J. and Patsis, P.A. 1998, *A&A*, 336, 840
- Heraudeau, P. and Simien, F. 1996, *A&AS*, 118, 111
- Ho, L. C., Filippenko, A. V., and Sargent, W. L. W. 1995, *ApJS*, 98, 477
- Keel, W. C. 1983, *ApJ*, 268, 632
- Kuijken, K., Merrifield, M.R. 1995, *ApJ*, 443, L13
- Matsuda, T., Inoue, M., Sawada, K., Shima, E., and Wakamatsu, K.-i. 1987, *MNRAS*, 229, 295
- Merrifield, M. R. and Kuijken, K. 1994, *ApJ*, 432, 575
- Moriondo, G., Giovanardi, C., and Hunt, L. K. 1998, *A&AS*, 130, 81
- Mulder, W. A. 1986, *A&A*, 156, 354
- Pfenniger, D. 1985, *A&A*, 150, 112

- Rots, A. H. 1980, *A&AS*, 41, 189
- Sil'chenko, O. K., Vlasyuk, V. V., and Burenkov, A. N. 1997, *A&A*, 326, 941
- Sofue, Y. and Wakamatsu, K.-i. 1994, *AJ*, 107, 1018
- Thornley, M. D. 1996, *ApJ*, 469, L45
- Thornley, M. D., and Mundy, L. G. 1997, *ApJ*, 484, 202
- Varela, A. M., Munoz-Tunon, C., and Simmoneau, E. 1996, *A&A*, 306, 381
- Vlasyuk, V. V. 1993, *Astrofiz. issled. (Izv. SAO RAS)* 36, 107
- Wagner, S. J., Dettmar, R.-J., and Bender, R. 1989, *A&A*, 215, 243
- Whitmore, B. C., Rubin, V. C., and Ford, W. K., Jr. 1984, *ApJ*, 287, 66
- Wozniak, H. and Pfenniger, D. 1997, *A&A*, 317, 14
- Zaritsky, D. and Lo, K. Y. 1986, *ApJ*, 303, 66

Fig. 1.— Radial distributions of ionized-gas line-of-sight velocities in $P.A. = 153^\circ$ (*a*) and in $P.A. = 145^\circ$ (*b*). A typical r. m. s. error of the velocities determined by searching for emission-line baricenters is 2 km/s, errors of the Gauss-analysis determinations are shown by vertical bars

Fig. 2.— The same as Fig. 1, but only for the central part of NGC 2841

Fig. 3.— *a* – Examples of correlation peaks from cross-correlation of galactic spectra in the spectral range of 8000–8840 ÅÅ with the spectra of template stars; two profiles, at $r = -40''$ (positive velocity shift) and at $r = +40''$ (negative velocity shift), are presented for the case $P.A. = 145^\circ$ and template star HR 3125; *b* – two autocorrelation peaks, HR 3125 *vs* HR 3125 and HR 3222 *vs* HR 3222

Fig. 4.— Radial distributions of stellar line-of-sight velocities in $P.A. = 153^\circ$ (*a*) and in $P.A. = 145^\circ$ (*b*); Gauss analysis has permitted us to extract three kinematical stellar subsystems over the whole radius range, the most intense contributor to the correlation peak at every radius is presented by enhanced signs

Fig. 5.— Isophotes of the surface brightness distributions in the emission lines H_α (*a*) and $[\text{NII}]\lambda 6583$ (*b*) for the central part of NGC 2841. North is up, east is to the left, the total size of the area shown is $29'' \times 29''$

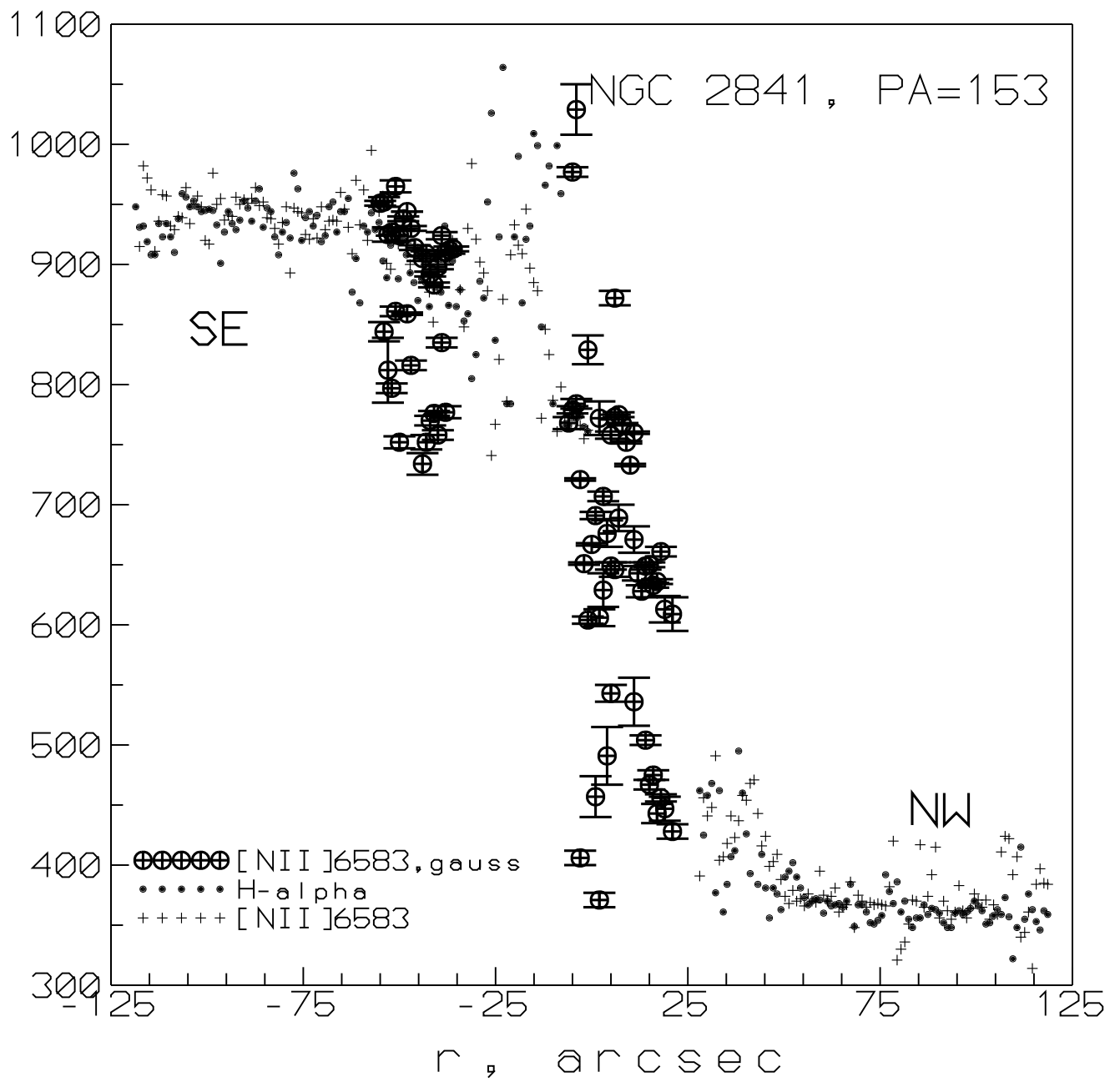
Fig. 6.— A map of $[\text{NII}]\lambda 6583$ -to- H_α flux ratio (grey-scaled) with the superimposed H_α surface brightness isophotes; the position angle of the top is 74° (north is to the right, east is up), the total sizes of the map are $2' \times 2'$

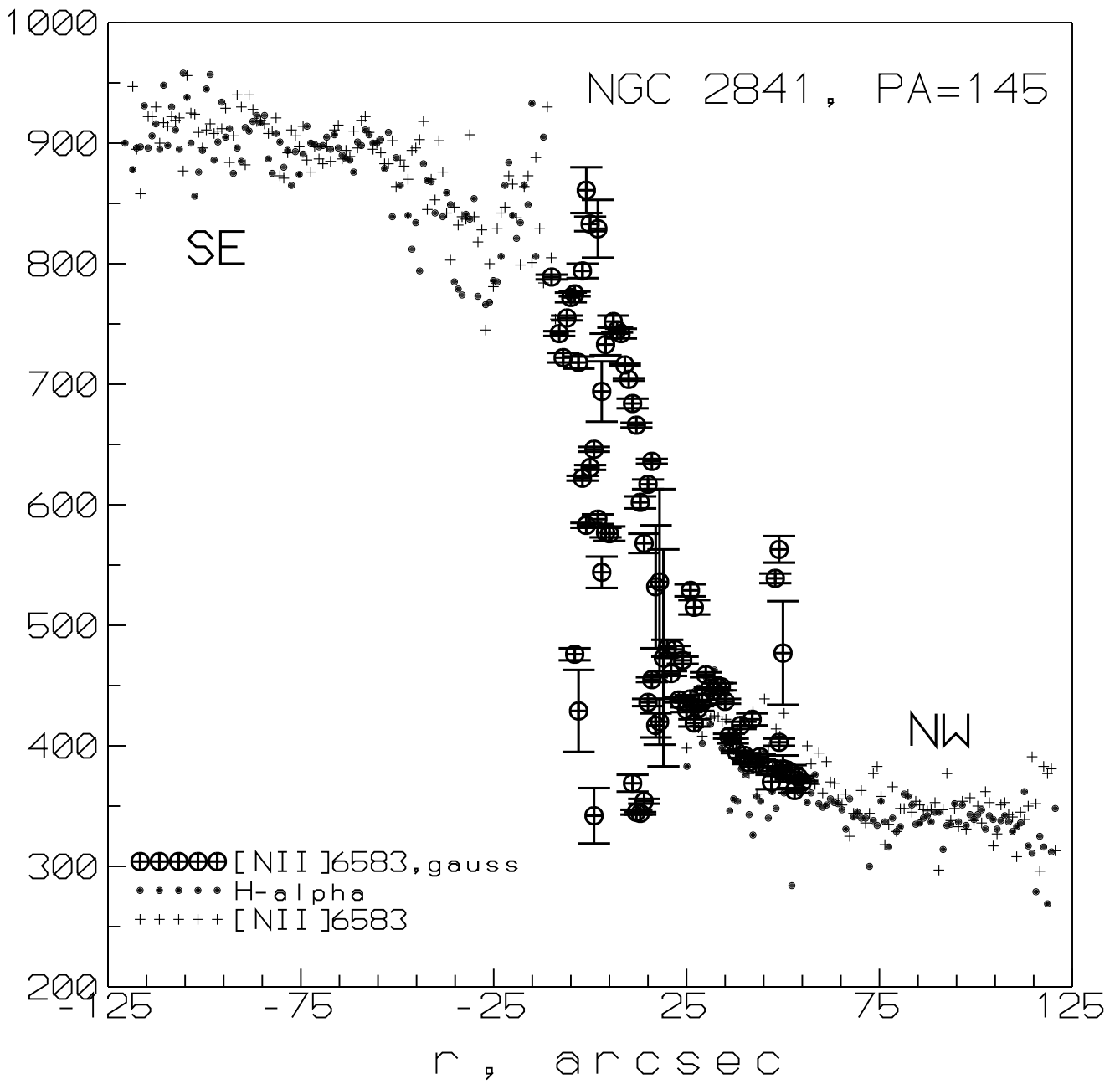
Fig. 7.— A piece of the Fig.1a in the radius range of $-20'' \div -80''$

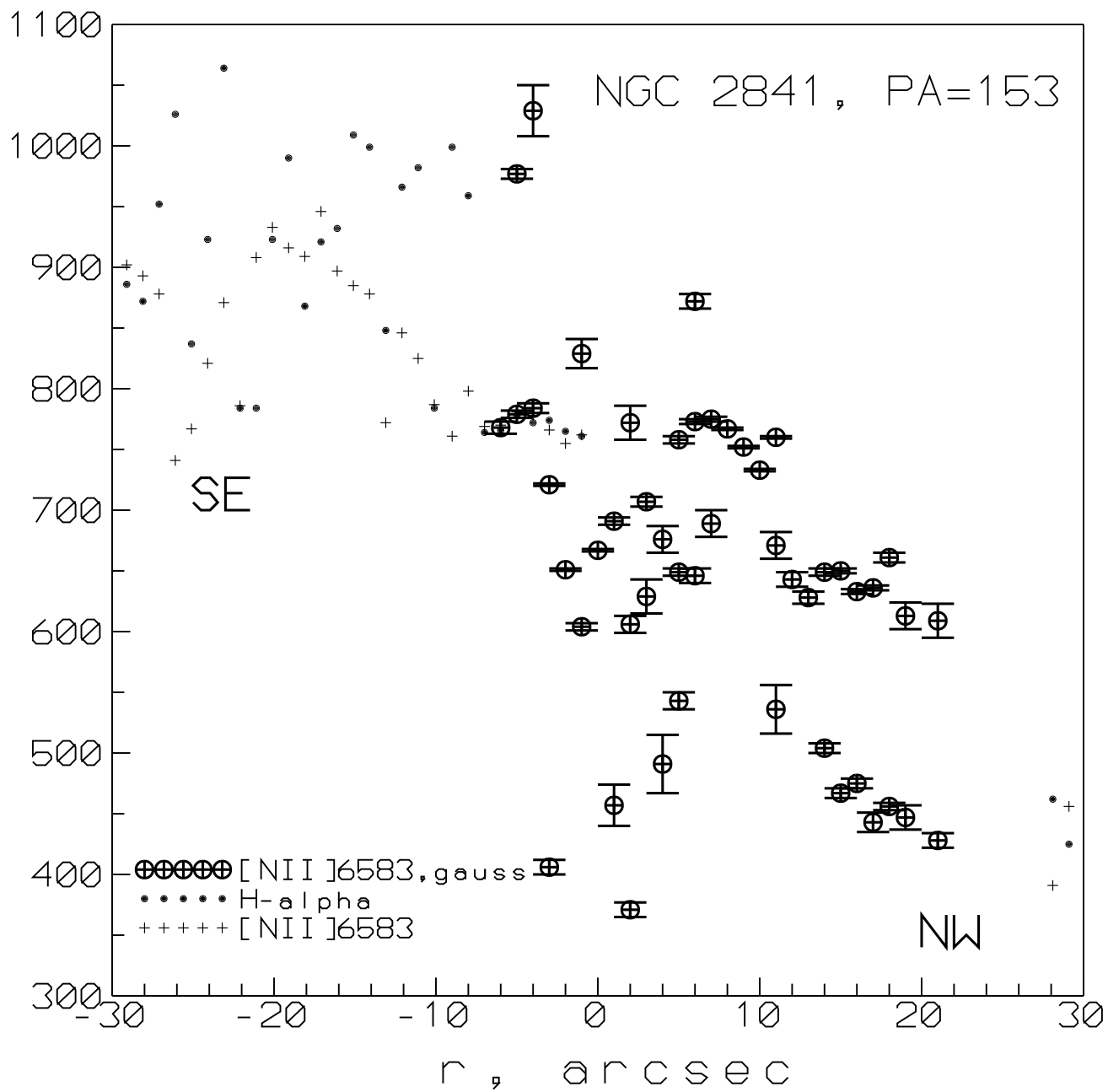
Fig. 8.— Results of the isophote analysis for the broad-band VRI images of the central part of NGC 2841: *a* — major axis position angle radial variations, *b* — ellipticity radial

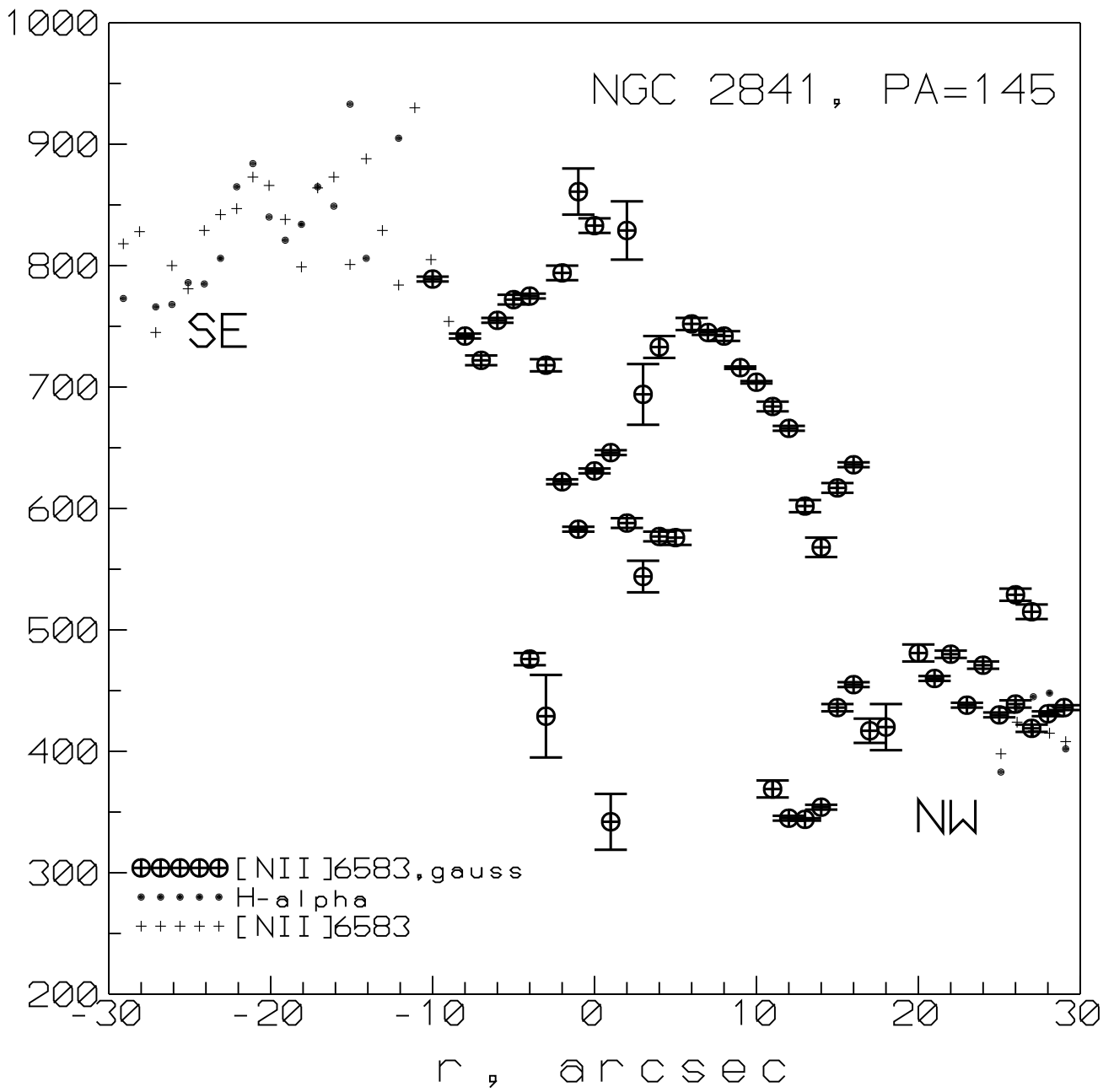
variations, c — boxiness radial variations; a fat straight line marks a proposed location of the large-scale bar in NGC 2841

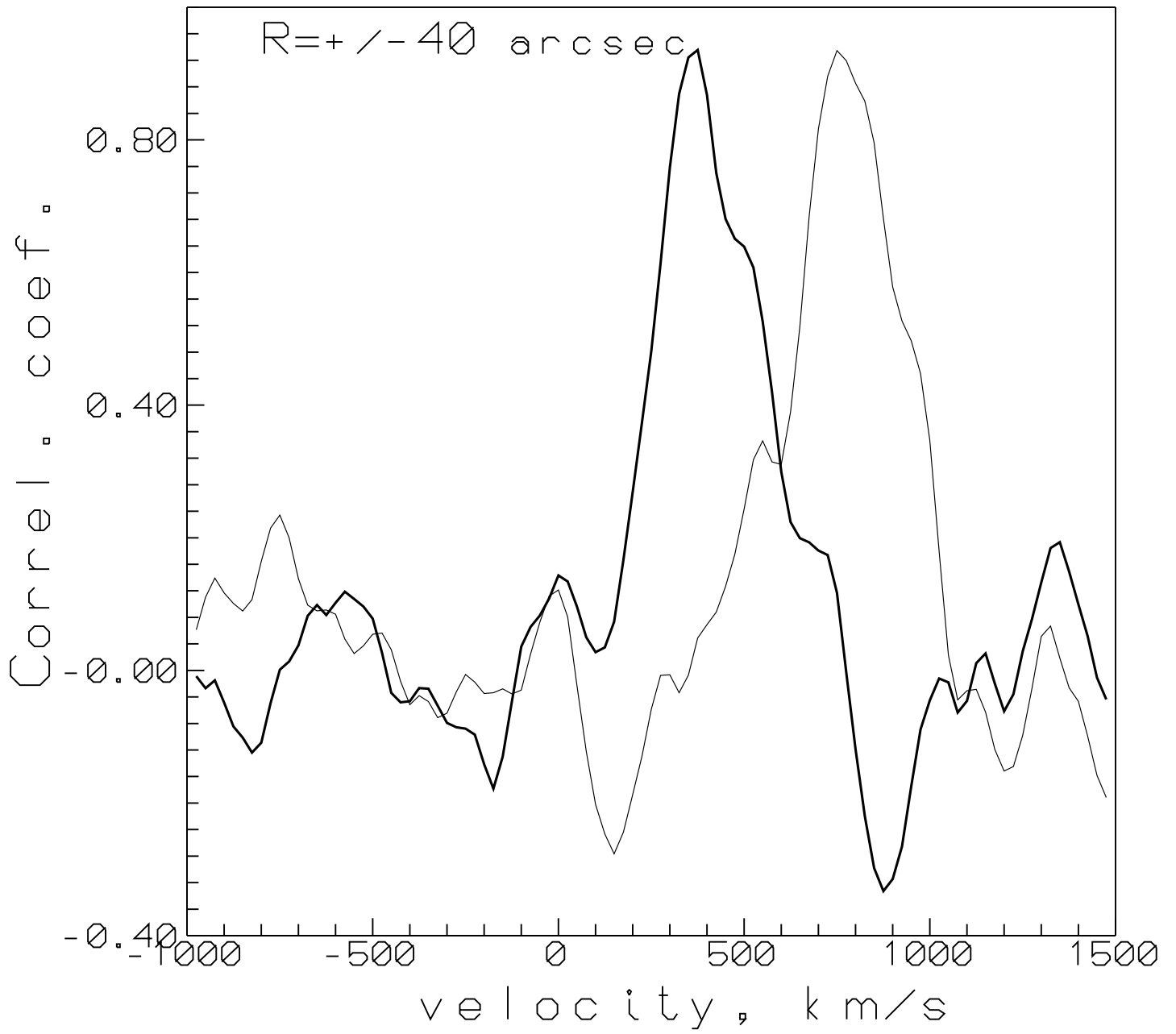
Fig. 9.— A scheme of the observational phenomena in NGC 2841; though the kinematical peculiarities (the gas on plane orbits orthogonal to the bar and stellar LOSVD multi-component structure) are observed mostly along the major axis, the two-dimensional areas are shaded for a better impression

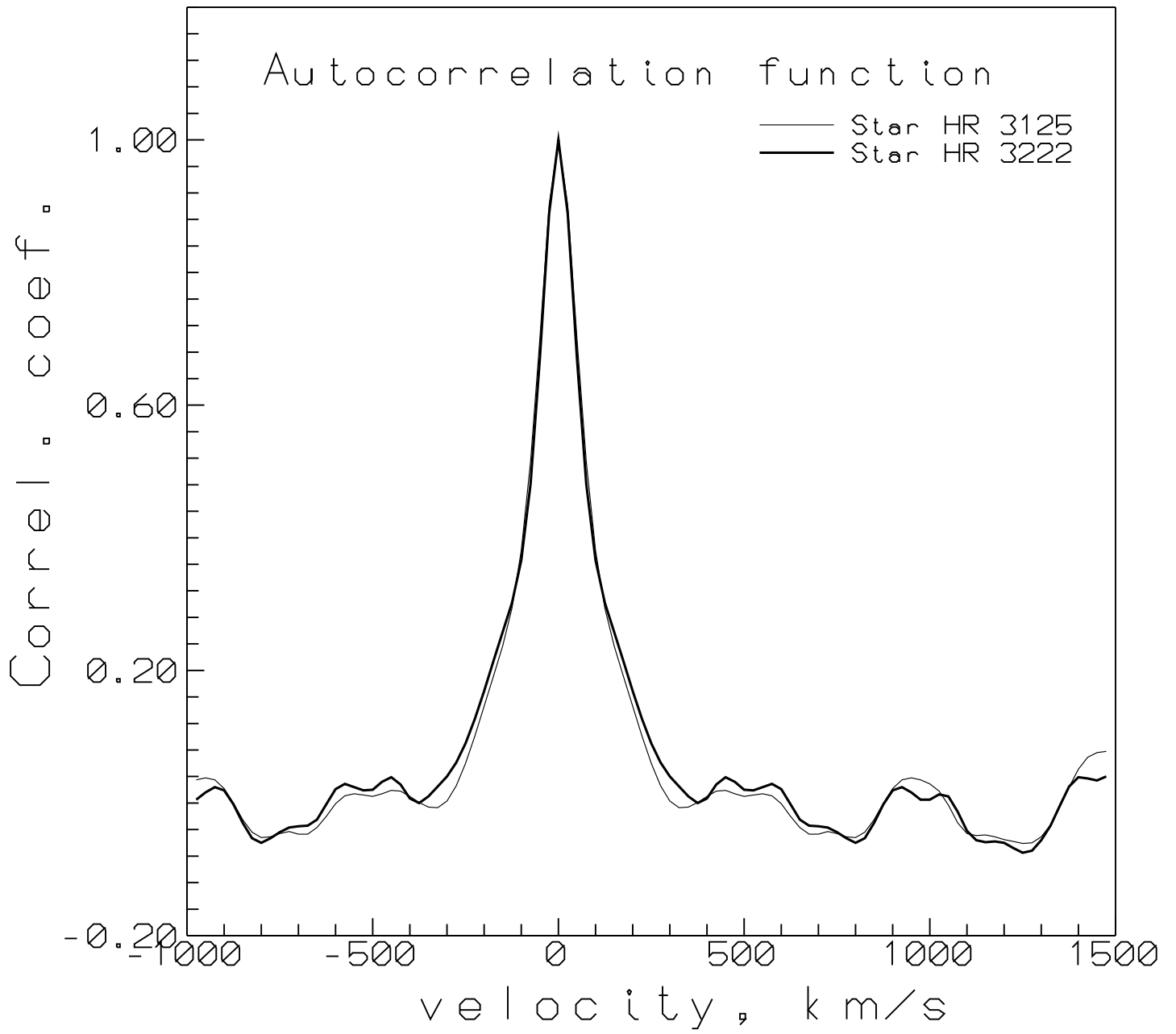




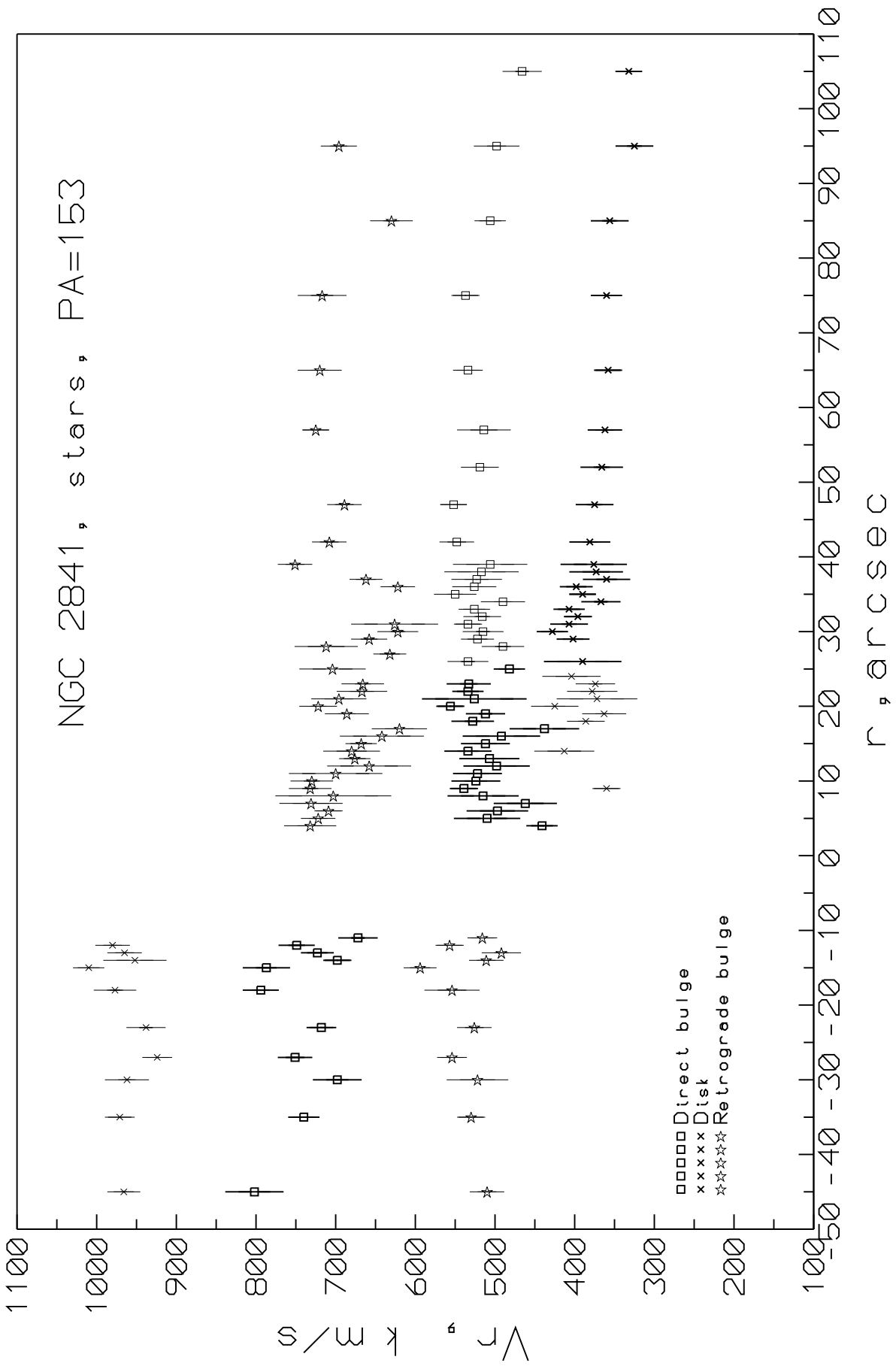








NGC 2841, stars, PA=153



NGC 2841, stars, PA=145

